NUCLEAR THEORY, Vol. 29 (2010)
eds. A. Georgieva, N. Minkov, Heron Press, Sofia

Proton Timelike Form Factors Near Threshold via Antiproton-Nucleus Electromagnetic Annihilation

V.A. Karmanov[1], **H. Fonvieille**[2]

[1]Lebedev Physics Institute, Leninsky prospekt 53, 119991 Moscow, Russia
[2]LPC, Université Blaise Pascal, IN2P3, 63177 Aubière Cedex, France

Abstract. In the reaction of the antiproton-deuteron electromagnetic annihilation $\bar{p} + d \to ne^+e^-$ the value of the invariant mass $M_{e^+e^-}$ of the e^+e^- pair can be near or below the $\bar{p}p$ mass even for enough high momentum of incident antiproton. This allows to access the proton electromagnetic form factors in the time-like region of q^2 near the $\bar{p}p$ threshold. We estimate the cross section $d\sigma(\bar{p} + d \to e^+e^-n)/dM_{e^+e^-}$ for an antiproton beam momentum of 1.5 GeV/c. We find that for values of $M_{e^+e^-}$ near the $\bar{p}p$ threshold this cross section is about 1 pb/MeV. The case of heavy nuclei ^{12}C, ^{56}Fe and ^{197}Au is also estimated. Elements of experimental feasibility are studied in the context of the $\overline{\mathrm{P}}\mathrm{ANDA}$ project [1, 2]. We conclude that this process has a chance to be measurable at $\overline{\mathrm{P}}\mathrm{ANDA}$.

1 Introduction

The electromagnetic form factors of the proton and the neutron are basic observables, which are the goal of extensive measurements. In the spacelike region, *i.e.*for a virtual photon four-momentum squared $q^2 < 0$, these form factors give information about the spatial distribution of electric charge and magnetization inside the nucleon. In the timelike region ($q^2 > 0$) they tell us about the dynamics of the nucleon-antinucleon ($N\bar{N}$) interaction.

The theoretical models, generally based on dispersion relations [3–5] or semi-phenomenological approaches [6,7], predict a smooth behavior of the form factor in the measured regions, but a peaked behavior in the timelike region below the $N\bar{N}$ threshold ($0 < q^2 < 4m^2$, m is the nucleon mass), due to poles in the amplitude (see *e.g.*Figure 1, taken from [8]). These poles are phenomenological inputs, built from meson exchange, and their properties are fitted to the data in the measured regions. The corresponding irregularities in form factors are related to the transition of $p\bar{p}$ to vector mesons which can decay in e^+e^- pair via a virtual photon.

The mesons with a mass near the $p\bar{p}$ mass can have a quasinuclear nature, *i.e.*, they can be formed by bound states and resonances in the $p\bar{p}$ system. Such vector mesons were predicted in the papers [9, 10]. Note that such mesons can

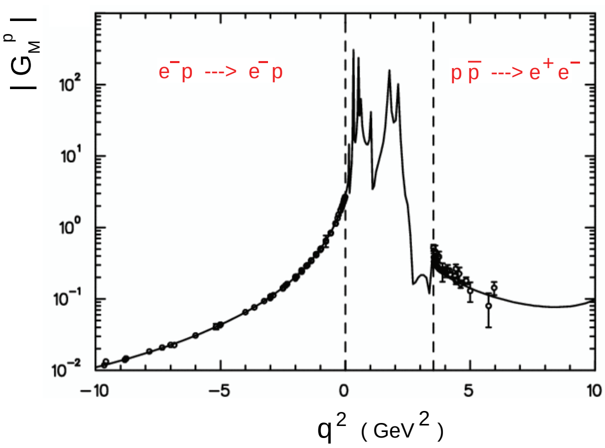

Figure 1. Experimental data and predictions for the magnetic proton form factor in the domain -10 GeV$^2 \leq q^2 \leq 10$ GeV^2. The figure is taken from [8].

be formed not only in the $p\bar{p}$ system but in $N\bar{N}$ in general and they can have not only vector quantum numbers. A review on quasinuclear mesons in the $N\bar{N}$ system is given in [11].

The under-threshold region ($0 < q^2 < 4m^2$) is called unphysical because it cannot be accessed experimentally by an on-shell process. Some experiments have been performed in the vicinity of the $N\bar{N}$ threshold, either in $p\bar{p} \to e^+e^-$ at LEAR [12] or in the inverse channel $e^+e^- \to p\bar{p}$ at Babar [13], but they cannot go below this physical threshold. However, a nucleus provides nucleons with various momenta, in modulus and direction, and also various degrees of off-shellness. Therefore it offers the possibility to produce an $N\bar{N}$ electromagnetic annihilation with an invariant mass squared $q^2 = s_{\bar{p}p}$ smaller than $4m^2$.

This possibility, which may give access to the proton form factors in the underthreshold region, for an off-shell nucleon, was explored in our paper [14]. The present talk is based on this paper.

The idea to use a nucleus for that purpose was explored in the 80's using deuterium [15]. The reaction is then:

$$\bar{p}\,d \to e^+e^-n \tag{1}$$

(a crossed-channel of deuteron electrodisintegration). The aim of the present paper is to revive this study in view of the future antiproton facility FAIR at GSI.

Other channels can give access to the off-shell nucleon form factors in the timelike region, including the underthreshold region; such processes have been studied theoretically in ref. [16] ($\gamma p \to pe^+e^-$) and in refs. [17, 18] ($\bar{p}p \to \pi^0e^+e^-$).

This paper is organized as follows: a theoretical study is presented in Section 2, experimental aspects are discussed in Section 3 and a conclusion is given in Section 4.

2 Theoretical Study

In elastic electron scattering from the nucleon $e^-N \to e^-N$ the momentum transfer squared $q^2 = (k-k')^2$ is always negative. This allows to measure the nucleon form factors in the space-like domain of q^2.

On the contrary, in the annihilation $N\bar{N} \to \gamma^* \to e^+e^-$ the mass of virtual photon is equal to the total c.m. $N\bar{N}$ energy. Its four-momentum squared is always greater than $4m^2$. This allows to measure the nucleon form factors in the time-like domain of q^2, above the $N\bar{N}$ threshold. In this reaction, in order to study the form factor behavior in a narrow domain near threshold, where non-trivial structures are predicted [11], one should have a beam of almost stopped antiprotons. This non-easy technical problem was solved at LEAR [12]. However, the under-threshold domain $0 \le q^2 \le 4m^2$ remains kinematically unreachable in this type of experiments.

One can penetrate in this domain of q^2 in the $\bar{p}$ annihilation on nuclei

$$\bar{p}A \to (A-1)\, e^+e^-,$$

see Figure 2. The symbol $(A-1)$ means not necessarily a nucleus but any system with the baryon number $A-1$. Since extra energy of the antiproton can be absorbed by the $(A-1)$ system, the e^+e^- pair may be emitted with very small invariant mass. Therefore the two-body reaction $\bar{p}A \to (A-1)\gamma^*$ is kinematically allowed for a very wide domain of invariant mass of the γ^*, which starts with two times the electron mass, namely:

$$4m_e^2 \le q^2 \le (\sqrt{s_{\bar{p}A}} - M_{A-1})^2 \, .$$

One can achieve near-threshold, under-threshold and even deep-under-threshold values of q^2 even for fast antiprotons. This however does not mean that this reaction provides us direct information about the nucleon form factors. For the

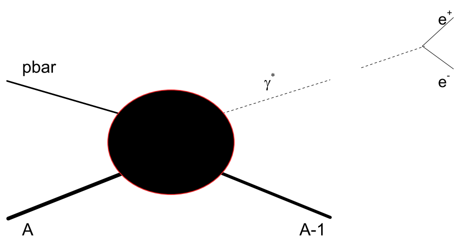

Figure 2. The process $\bar{p}A \to (A-1)\gamma^*$ (followed by $\gamma^* \to e^+e^-$).

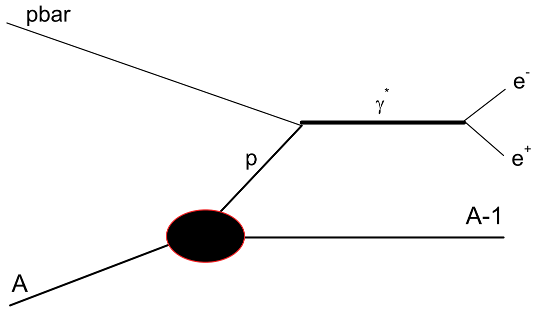

Figure 3. Amplitude of the reaction $\bar{p}A \to (A-1)\gamma^*$ in impulse approximation.

latter, we should be sure that the observed e^+e^- pair (and nothing more) was created in the annihilation $\bar{p}p \to e^+e^-$ on the proton in the nucleus, *i.e.*, that the reaction mechanism is given by the diagram of Figure 3 or by a similar diagram where the $\bar{p}$ can rescatter before annihilation.

At the same time, since the nucleons in the nucleus are off-mass-shell, the form factors entering the amplitude of Figure 3, are not precisely the same as found in the free $\bar{p}p$ annihilation. In general, the three-leg vertex $F = F(p_1^2, p_2^2, q^2)$ depends not only on the photon virtuality q^2, but also on the nucleon ones p_1^2, p_2^2. In the case considered, the incident antiproton is on-energy-shell: $p_{\bar{p}}^2 = m^2$, however the form factors depend on the proton virtuality p_p^2. How the form factor $F(p_{\bar{p}}^2 = m^2, p_p^2 \neq m^2, q^2)$ *vs.*q^2 differs from the free one $F(p_{\bar{p}}^2 = m^2, p_p^2 = m^2, q^2)$ – this depends on the dynamics determining its behavior *vs.*the nucleon leg virtuality. The nucleon form factors with off-shell nucleons were studied in the papers [19, 20]. Generally, we can expect that the form factor dependence *vs.*p_p^2 is much smoother than the q^2 dependence. The p_p^2 dependence can be determined by the nucleon self-energy corrections (*i.e.*, by the structure of the nucleon), whereas the q^2 dependence in the time-like domain is governed by the $\bar{p}p$ interaction. The nucleon dynamics has a much larger energy scale than the nuclear one. The typical off-shell variation found in the papers [19, 20] was from a few to 10 percent. We do not pretend to such an accuracy here. Therefore we neglect this effect in our calculation. We will come to this question later. In any case, both domains: $q^2 < 4m^2,\ p_p^2 = m^2$ and $q^2 < 4m^2,\ p_p^2 < m^2$ are totally unexplored experimentally and are interesting and intriguing.

We emphasize that though the form factor dependence on p_p^2 can be weak, the nucleon off-mass-shell effect is very important for the kinematical possibility to reach the near- and under-threshold domain of q^2 with fast antiprotons. To produce the near-threshold e^+e^- pairs in annihilation of a fast $\bar{p}$ on an on-mass-shell proton, the antiproton should meet in the nucleus a fast proton with parallel momentum. The probability of that, which was estimated in the Glauber approach, is negligibly small relative to the results presented below. However, if the effective mass p_p^2 of the virtual proton is smaller than m^2 (that is just the case in a nucleus), then the near- and under-threshold e^+e^- pairs can be produced in collisions with not so fast intra-nucleus nucleons. This effect considerably increases the cross section. To have an idea of the order of magnitude which one can expect for this cross section, we will calculate it in the impulse approximation. Numerical applications will be done for the lowest antiproton beam momentum foreseen in future projects. Namely, at the High Energy Storage Ring at FAIR-GSI this value is 1.5 GeV/c.

2.1 Cross Section Calculation

At first, we consider the case of the deuteron target. If we know the amplitude of the reaction $\bar{p}d \to e^+e^-n$: $M_{\bar{p}d\to e^+e^-n}$ (to be calculated below), then the corresponding cross section is given by:

$$d\sigma_{\bar{p}d\to e^+e^-n} = \frac{(2\pi)^4}{4I}|M_{\bar{p}d\to e^+e^-n}|^2 \tag{2}$$

$$\times\delta^{(4)}(p_{\bar{p}} + p_d - p_{e^+} - p_{e^-} - p_n)\frac{d^3p_{e^+}}{(2\pi)^3 2\epsilon_{e^+}}\;\frac{d^3p_{e^-}}{(2\pi)^3 2\epsilon_{e^-}}\;\frac{d^3p_n}{(2\pi)^3 2\epsilon_n}$$

where I results from the flux factors. Here and below we imply the sum over the final spin projections and average over the initial ones.

Our estimations are carried out in the impulse approximation, when the mechanism is given by the diagram of Figure 3. Then the total amplitude squared $|M_{\bar{p}d\to e^+e^-n}|^2$ is proportional to the annihilation amplitude squared $|M_{\bar{p}p\to e^+e^-}|^2$ and to the square of the deuteron wave function $|\psi|^2$:

$$|M_{\bar{p}d\to e^+e^-n}|^2 = 4m\,|M_{\bar{p}p\to e^+e^-}|^2\;|\psi|^2, \tag{3}$$

and $|\psi|^2$ is normalized to 1.

We are interested in the distribution in the invariant mass $\mathcal{M}$ of the final e^+e^- system. To find it, for fixed value of $\mathcal{M}$, we can integrate, in some limits, over the angles of the recoil neutron (determining the neutron recoil momentum) and over the angles of the emitted e^+e^- in their center of mass. This can be done using standard phase volume techniques. The derivation is presented in detail in [14]. The final result reads:

$$\frac{d\sigma_{\bar{p}d\to e^+e^-n}}{d\mathcal{M}} = \sigma_{\bar{p}p\to e^+e^-}(\mathcal{M})\;\eta(\mathcal{M}), \tag{4}$$

where $\eta(\mathcal{M})$ is the distribution (given by eq. (6) below) of the e^+e^- invariant mass $\mathcal{M}$ and $\sigma_{\bar{p}p\to e^+e^-}(\mathcal{M})$ is the cross section of the $\bar{p}p \to e^+e^-$ annihilation at the total energy $\mathcal{M}$.

The calculation of $\sigma_{\bar{p}p\to e^+e^-}$ is standard. To estimate the nuclear effect, we omit the nucleon electromagnetic form factors. Then the $\bar{p}p \to e^+e^-$ cross section obtains the form:

$$\sigma_{\bar{p}p\to e^+e^-} = \frac{2\alpha^2\pi(2m^2+\mathcal{M}^2)}{3\mathcal{M}^2 m p_{\bar{p},lab}} \,. \tag{5}$$

Though $\sigma_{\bar{p}p\to e^+e^-}$ depends on $\mathcal{M}$, the main (nuclear) effect is determined by the factor $\eta(\mathcal{M})$ [14]:

$$\eta(\mathcal{M}) \;\; = \;\; \frac{m p^*_{\gamma^* n}\mathcal{M}}{(2\pi)^2\sqrt{s_{\bar{p}d}}} \int_{-1}^{1} |\psi(k)|^2 dz. \tag{6}$$

Here $z = \cos\theta$, where θ is the angle, in the c.m. frame of the reaction, between the initial deuteron momentum $\vec{p}^{\,*}_d$ and the final neutron momentum $\vec{p}^{\,*}_n$. The argument of the wave function k depends on z. This explicit dependence is given in [14].

Since, as mentioned, the wave function squared $|\psi(k)|^2$ is normalized to 1, the distribution $\eta(\mathcal{M})$ is also automatically normalized to 1:

$$\int_0^\infty \eta(\mathcal{M}) d\mathcal{M} = 1. \tag{7}$$

The total cross section is obtained by integrating (4) in the finite limits $\mathcal{M}_{min} \leq \mathcal{M} \leq \mathcal{M}_{max}$, where $\mathcal{M}_{min} = 2m_e$, $\mathcal{M}_{max} = \sqrt{s_{\bar{p}d}} - m$. Neglecting the electron mass, we can put $\mathcal{M}_{min} = 0$. For $p_{\bar{p},lab} = 1.5$ GeV/c the value $\mathcal{M}_{max}$ is high enough and provides the normalization condition (7) with very high accuracy.

To emphasize more distinctly the effect of the nuclear target, we can represent the cross section (5) of the annihilation $\bar{p}p \to e^+e^-$ on a free proton similarly to eq. (4):

$$\frac{d\sigma_{\bar{p}p\to e^+e^-}}{d\mathcal{M}} = \sigma_{\bar{p}p\to e^+e^-}\delta(\mathcal{M} - \sqrt{s_{p\bar{p}}}) \tag{8}$$

where $\sigma_{\bar{p}p\to e^+e^-}$ is defined in (5), $s_{p\bar{p}} = (p_p + p_{\bar{p}})^2$. The fact that in the annihilation on a free proton the mass of the final e^+e^- pair is fixed is reflected in (8) in the presence of the delta-function. Comparing this formula with (4), we see that the effect of the nuclear target results in a dilation of the infinitely sharp distribution $\delta(\mathcal{M} - \sqrt{s_{p\bar{p}}})$ in a distribution of finite width $\eta(\mathcal{M})$. The dilation of a distribution does not change its normalization: $\eta(\mathcal{M})$ remains normalized to 1.

2.2 Analysis and Numerical Calculations

At first glance, the small near-threshold $\bar{p}p$ c.m. energy $\mathcal{M} \approx 2m$ in the collision of a fast $\bar{p}$ ($p_{\bar{p}} = 1500$ MeV/c) is achieved, when the antiproton meets in the deuteron a fast proton having the same momentum as the $\bar{p}$, in modulus and direction. The protons with such a high momentum are very seldom in deuteron.

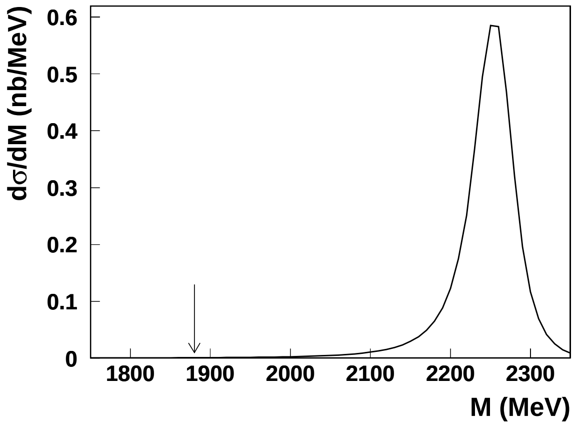

Figure 4. The cross section $\frac{d\sigma_{\bar{p}d\to e^+e^-n}}{d\mathcal{M}}$ of the reaction $\bar{p}d \to e^+e^-n$ *vs.*$\mathcal{M}$, in the interval: 1750 MeV $\leq \mathcal{M} \leq 2350$ MeV, calculated for a pointlike proton. The arrow indicates the $p\bar{p}$ threshold.

For this mechanism, the cross section would be very small. However, the near-threshold value of $\mathcal{M}$ is obtained in other kinematics. As we mentioned, the proton momenta k in the deuteron wave function $\psi(k)$ in eq. (6) start with $k \approx k_{min} \approx 360$ MeV/c only (that corresponds to $z \approx 1$). The main reason which allows to obtain in this collision the value $\mathcal{M} \approx 2m$ is the off-shellness of the proton: $m^* \leq 0.85m$ instead of $m^* = m$. This 15% decrease relative to the free proton mass is enough to obtain the invariant $p\bar{p}$ mass $\mathcal{M} \approx 2m$, when one has the two parallel momenta: 1500 MeV/c for $\bar{p}$ and 360 MeV/c for p.

The cross section $d\sigma_{\bar{p}d\to e^+e^-n}/d\mathcal{M}$, eq. (4), has been calculated for an antiproton of momentum $p_{\bar{p}} = 1500$ MeV/c on a deuteron nucleus at rest, with the deuteron wave function [21], incorporating two components corresponding to S- and D-waves. The result is shown in Figure 4. The maximum of the cross section is at $\mathcal{M} = 2257$ MeV, that corresponds to the $\bar{p}$ interacting with a proton at rest (and on-shell). The cross section integrated over $\mathcal{M}$ is equal to 43 nb. We remind that these calculations do not take into account the proton form factor. Its influence will be estimated below. The numerical integral over $\mathcal{M}$ of the function $\eta(\mathcal{M})$, eq. (6), is ≈ 1, in accordance with the normalization condition (7).

The $p\bar{p}$ threshold value $\mathcal{M} = 1880$ MeV is on the tail of the distribution, far from the maximum. Relative to the maximum, the cross section at threshold decreases approximately by a factor 600. The numerical value at the threshold is:

$$\left.\frac{d\sigma}{d\mathcal{M}}\right|_{\mathcal{M}=2m} = 1\ \frac{pb}{\text{MeV}}\ . \tag{9}$$

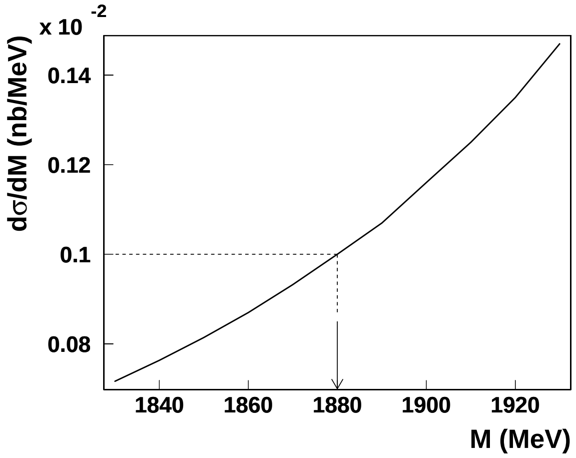

Figure 5. The same as in Figure 4, but near the $p\bar{p}$ threshold, in the interval 1830 MeV $\leq$ $\mathcal{M} \leq 1930$ MeV.

In Figure 5 this cross section is shown in the near-threshold interval 1830 MeV $\leq$ $\mathcal{M} \leq 1930$ MeV. The integral over $\mathcal{M}$ in a bin of width 100 MeV centered on the threshold is:

$$\int_{1830\ MeV}^{1930\ MeV} \frac{d\sigma_{\bar{p}d\to e^+e^-n}}{d\mathcal{M}}\ d\mathcal{M} \approx 100\ pb\ .$$

These estimations take into account the suppression resulting from the momentum distribution in deuteron. However, they do not incorporate the form factors of the nucleon. To incorporate them in a simplified way, one can consider an effective form factor $|F|$ which depends on $\mathcal{M}$, and include it in the integral:

$$\sigma_{\bar{p}d\to e^+e^-n} = \int \sigma_{\bar{p}p\to e^+e^-}(\mathcal{M})\ \eta(\mathcal{M})\ |F(\mathcal{M})|^2 d\mathcal{M} \tag{10}$$

where $\sigma_{\bar{p}p\to e^+e^-}(\mathcal{M})$ is the cross section for pointlike nucleons given in eq.(5). To have an estimate of this integral, we have taken the effective proton form factor measured in ref. [13]. By doing this, we neglect all off-shell effects. We interpolate $|F(\mathcal{M})|$ linearly between the measured values, and we limit the integral to the region $\mathcal{M} \geq 2m$. In this way we obtain $\sigma_{\bar{p}d\to e^+e^-n} \simeq 1$ nb, which is comparable to the total cross section $\sigma_{\bar{p}p\to e^+e^-}$ on a free proton at $\mathcal{M} = 2257$ MeV. We point out that at threshold, our differential cross section $d\sigma_{\bar{p}d\to ne+e-}$ of 1 pb/MeV (eq. (9)) is not suppressed by any factor, since there the form factor $|F|$ seems to be close to 1 experimentally [22, 23]. Below this threshold one may expect a form factor effect *larger* than one.

2.3 Annihilation on Heavier Nuclei

For $A > 2$, we should take into account the possibility of excitation and breakup of the final nucleus $A - 1$ in the process $\bar{p}A \to (A-1)\gamma^*$. The result contains the sum over the final energies of the residual nucleus and the integral over a continuous spectrum. That is, the function $|\psi(k)|^2$ in eq. (6) is replaced by the integral $\int_{E_{min}}^{E_{max}} S(E,k)dE$, where $S(E,k)$ is the nucleus spectral function giving the probability to find in the final state the nucleon with the relative momentum k and the residual nucleus with energy E. For high incident energy we can replace the upper limit by infinity. Then we obtain:

$$\int_{E_{min}}^{\infty} S(E,k)dE = n(k),$$

where $n(k)$ is the momentum distribution in the nucleus.

To estimate the cross section on heavy nuclei, we will still use eqs. (4), (6) but with the two following changes. (*i*) We replace the deuteron momentum distribution by the nuclear one. (*ii*) We multiply (6) by the number of protons Z.

The numerical calculations were carried out for the ^{12}C, ^{56}Fe and ^{197}Au nuclei with the nuclear momentum distributions found in the papers by A.N. Antonov *et al.*: [24, 25]. Near threshold, *i.e.*at $\mathcal{M} = 1880$ MeV, for all three nuclei we obtain very close results given by (compare with eq. (9) for deuteron):

$$\frac{d\sigma_{\bar{p}A\to e^+e^-X}}{d\mathcal{M}} \approx 6.5\, Z\, \frac{pb}{MeV} \tag{11}$$

Multiplying by the charge Z ($Z(^{12}\text{C}) = 6$, $Z(^{56}\text{Fe}) = 26$, $Z(^{197}\text{Au}) = 79$) and integrating (11) over a 1 MeV interval near $\mathcal{M} = 1880$ MeV, we get:

$$\sigma(^{12}\text{C}) = 39\; pb,\;\; \sigma(^{56}\text{Fe}) = 0.17\; nb,\;\; \sigma(^{197}\text{Au}) = 0.5\; nb.$$

These results were obtained without taking into account the absorption of $\bar{p}$ in nucleus before electromagnetic annihilation. This absorption was estimated in Glauber approach. It reduces these cross sections by only a factor 2.

2.4 Beyond the Impulse Approximation

There exist other possible mechanisms for the process $\bar{p}\,d \to e^+e^-n$. One of them is the initial state interaction, which includes rescattering (not only elastic) of the initial $\bar{p}$ in the target nucleus. In the rescattering, the incident $\bar{p}$ looses energy and therefore the proton momentum needed to form the invariant mass $\mathcal{M} \approx 2m$ becomes smaller. The probability to find such a proton in deuteron is higher. Therefore initial state interaction increases the cross section.

Other processes are discussed in [14]. We emphasize that in any case, whatever the intermediate steps are in process (1), the e^+e^- pair of the final state must come necessarily from the baryon-antibaryon electromagnetic annihilation, $\bar{p}p$ or $\bar{n}n$, because there is only one neutron left at the end. It cannot come from another process, even if there are complicated intermediate steps, like rescattering, etc. Therefore this e^+e^- pair is a direct and very little distorted probe of the baryon-antibaryon electromagnetic annihilation vertex.

3 Experimental Aspects

Experimental aspects have been investigated in detail in [14] in the case of a deuteron target, *i.e.*for the three-body process $\bar{p}\,d \to e^+e^-n$, in the conditions of the $\overline{\mathrm{P}}\mathrm{ANDA}$ project at FAIR-GSI: an antiproton beam momentum of 1.5 GeV/c and the detection of the lepton pair. The count rate in the near-threshold region of $\mathcal{M}$ is small but not negligible. The main difficulty is to identify the reaction among the hadronic background which is about six orders of magnitude higher. First elements of strategy were presented for this background rejection, based on particle identification, detector hermeticity, and missing mass resolution.

One should also also note that the luminosity in ($\bar{p}$A) decreases with the atomic charge Z of the target nucleus [1], in a way that roughly compensates the increase of cross section with Z reported in sect. 2.3.

Although the subject would require a much more detailed study, it was concluded that this process has a chance to be measurable in $\overline{\mathrm{P}}\mathrm{ANDA}$, given the very good design performances of the detector.

The antiproton momentum 1.5 GeV/c just corresponds to the threshold value of creation of the $\Lambda\bar{\Lambda}$ pair on a free proton. Therefore the virtual creation of the $\Lambda\bar{\Lambda}$ pair in reaction (1) is not suppressed by the nucleon momentum distribution in deuteron and contributes just in the domain of the peak of Figure 4, that allows one to study the $\Lambda\bar{\Lambda}$ threshold region with good statistics. In the $\Lambda\bar{\Lambda}$ system, the quasi-nuclear states were predicted in [26] and, similarly to the $N\bar{N}$ quasi-nuclear states, they should manifest themselves as irregularities in the cross section. The contribution of the channel $\bar{p}p \to \bar{\Lambda}\Lambda \to e^+e^-$ in the total cross section $\bar{p}p \to e^+e^-$ (the latter equals 1 nb, see sect. 2.2 above) was estimated in [27] as 0.1 nb, *i.e.*10% of the total cross section. Therefore we expect that the structures caused by the channel $\bar{p}p \to \bar{\Lambda}\Lambda \to e^+e^-$ can be observed in process (1) in the region of mass $\mathcal{M}$ near the $\Lambda\bar{\Lambda}$ threshold.

4 Conclusion

We have studied the reaction $\bar{p}A \to (A-1)\gamma^*$ (followed by $\gamma^* \to e^+e^-$). This process gives access to the $\bar{p}p$ annihilation $\bar{p}p \to \gamma^*$ at invariant masses $\sqrt{s}_{\bar{p}p}$ which are below the physical threshold of $2m$, due to the proton off-shellness in the nucleus. In this way a possibility exists to access the proton timelike form factors in the near-threshold and the totally unexplored under-threshold region, where $N\bar{N}$ bound states are predicted.

The differential cross section $d\sigma/d\mathcal{M}$ has been calculated as a function of the dilepton invariant mass $\mathcal{M}$, for an incident antiproton of 1.5 GeV/c momentum on a deuteron target (and heavier nuclei). We find that the $p\bar{p}$ threshold

($\mathcal{M} = 2m$) is reached for a minimal proton momentum $k_{\min}$=360 MeV/c in the nucleus, and at this point the cross section is about 1 pb/MeV.

The estimations carried out above show that this process has a chance to be measurable in $\overline{\mathrm{P}}\mathrm{ANDA}$, provided the very good design performances of the detector.

References

[1] The PANDA Collaboration, *Physics Performance Report for PANDA: Strong Interaction Studies with Antiprotons* arXiv:0903.3905 [hep-ex].

[2] The PANDA Collaboration, *Technical Progress Report for PANDA* (2005) http://www-panda.gsi.de/archive/public/ panda_tpr.pdf

[3] R. Baldini, *et al.*, *Eur. Phys. J. C* **11** (1999) 709–715.

[4] H. W. Hammer, U.-G. Meissner, D. Drechsel, *Phys. Lett. B* **385** (1996) 343–347.

[5] C. Adamuscin, S. Dubnicka, A. Z. Dubnickova, P. Weisenpacher, *Prog. Part. Nucl. Phys.* **55** (2005) 228–241.

[6] F. Iachello, Q. Wan, *Phys. Rev. C* **69** (2004) 055204.

[7] R. Bijker, F. Iachello, *Phys. Rev. C* **69** (2004) 068201.

[8] U.-G. Meissner, *Nucl. Phys. A* **666** (2000) 51–60.

[9] O. D. Dalkarov, K. V. Protasov, *Nucl. Phys. A* **504** (1989) 845–854.

[10] O. D. Dalkarov, K. V. Protasov, *Mod. Phys. Lett. A* **4** (1989) 1203.

[11] I. S. Shapiro, *Phys. Rept.* **35** (1978) 129–185.

[12] G. Bardin, *et al.*, *Nucl. Phys. B* **411** (1994) 3–32.

[13] B. Aubert, *et al.*, *Phys. Rev. D* **73** (2006) 012005.

[14] H. Fonvieille and V.A. Karmanov, *Eur. Phys. J. A* **42** (2009) 287–298.

[15] O. D. Dalkarov, V. G. Ksenzov, *JETP Lett.* **31** (1980) 397-400.

[16] M. Schafer, H. C. Donges, U. Mosel, *Phys. Lett. B* **342** (1995) 13–18.

[17] C. Adamuscin, E. A. Kuraev, E. Tomasi-Gustafsson, F. E. Maas, *Phys. Rev. C* **75** (2007) 045205.

[18] A. Z. Dubnickova, S. Dubnicka, M. P. Rekalo, *Z. Phys. C* **70** (1996) 473–482.

[19] H. W. L. Naus, J. H. Koch, *Phys. Rev. C* **36** (1987) 2459–2465.

[20] P. C. Tiemeijer, J. A. Tjon, *Phys. Rev. C* **42** (1990) 599–609.

[21] J. Carbonell, V. A. Karmanov, *Nucl. Phys. A* **581** (1995) 625–653.

[22] R. Baldini, S. Pacetti, A. Zallo, A. Zichichi, *Eur. Phys. J. A* **39** (2009) 315–321.

[23] R. Baldini, S. Pacetti, A. Zallo, arXiv:0812.3283 [hep-ph].

[24] A.N. Antonov, M.K. Gaidarov, M.V. Ivanov, D.N. Kadrev, E. Moya de Guerra, P. Sarriguren, J.M. Udias, *Phys. Rev. C* **71** (2005) 014317.

[25] A.N. Antonov, M.V. Ivanov, M.K. Gaidarov, E. Moya de Guerra, J.A. Caballero, M.B. Barbaro, J.M. Udias, P. Sarriguren, *Phys. Rev. C* **74** (2006) 054603.

[26] J. Carbonell, K. V. Protasov, O. D. Dalkarov, *Phys. Lett. B* **306** (1993) 407–410.

[27] O. D. Dalkarov, *private communication.*